ELSEVIER

Journal of Photochemistry and Photobiology A: Chemistry 136 (2000) 235–240

Journal of Photochemistry and Photobiology A:Chemistry

www.elsevier.nl/locate/jphotochem

Photoassisted degradation of dyes in the presence of Fe^{3+} and H_2O_2 under visible irradiation

Yinde Xie [a], Feng Chen [a], Jianjun He [a], Jincai Zhao [a,*], Hui Wang [b]

[a] *The Laboratory of Photochemistry, Center for Molecular Science, Institute of Chemistry, Chinese Academy of Sciences, Beijing 100101, China*
[b] *Department of Environmental Engineering, Tsinghua University, Beijing 100084, China*

Received 17 April 2000; received in revised form 26 June 2000; accepted 18 July 2000

Abstract

The homogeneous photocatalytic degradation of cationic acridine orange monohydrochloride (AO) and anionic alizarin violet 3B (AV) in photo-Fenton system under visible irradiation was studied. The generated intermediates and degradation processes of AO were investigated by EPR, IR and GS–MS. It was found that visible irradiation not only enhances apparently the generation of hydroxyl radicals but also accelerates effectively the degradation of the dyes in the presence of Fe^{3+} and H_2O_2. *N*,*N*-dimethyl formaldehyde and *N*,*N*-dimethyl acetamide were found during the degradation of AO. Ammonium ions were also formed during the degradation of AO through the ion-selective electrode analysis.

Keywords: Acridine orange monohydrochloride; Alizarin violet 3B; Photo-Fenton; Degradation; EPR

1. Introduction

More than one century ago, Fenton discovered that the mixture of ferrous ion and hydrogen peroxide can oxidize many organic compounds that was called Fenton reaction later on. Since the reaction is not only very simple but also the Fe^{3+} or Fe^{2+} are easily treated by coagulation method, the Fenton reaction is widely used in many fields such as degradation of pollutants. Recently, the system Fe^{3+}(or Fe^{2+})/H_2O_2/$h\nu$ (photo-Fenton) has attracted much attention, and some studies have been reported on the photodegradation of pollutants such as anisole [1], phthalate [2], anthroquinone [3], lindane [4], quinoline [5], xylidine [6,7], phenols [8–11], Orange-II [12], chlorophenoxy herbicide [13], in which UV light was used.

As we know that the most important step of the photodegradation under UV light irradiation is the production of hydroxyl radicals and the regeneration of Fe^{2+} in photo-Fenton degradation, since under UV irradiation $Fe(OH)^{2+}$ ions can be excited and further generate additional hydroxyl radicals (Eq. (1)). Hydroxyl radical is a powerful oxidant that can be used to oxidize many organic contaminants into carbon dioxide and water [14]

$$Fe(OH)^{2+} \rightarrow Fe^{3+} + HO^{\bullet} \quad (\text{UV irradiation}) \tag{1}$$

$$Fe^{2+} + H_2O_2 \rightarrow Fe^{3+} + OH^- + HO^{\bullet}, \quad k_1 = 76 \pm 1.9\,M\,s^{-1} \tag{2}$$

Because the maximum absorption wavelength of $Fe(OH)^{2+}$ species is less than 400 nm, visible irradiation (>470 nm in our experiments) may not drive the reaction of Eq. (1). The majority of the sunlight is visible light; therefore, it must be of importance in the environmental field that utilize visible light to degrade pollutants. Similarly, the deep exploration of the nature of the photo-Fenton degradation, however, is of much importance no matter what is the application of this technology or the theoretical study of the photo-Fenton reaction.

Acridine orange is a heterocyclic dye containing nitrogen atoms, which is widely used in the fields of printing and dyeing, leather, printing ink and lithography. It is a serious pollutant in wastewater, meanwhile difficult to be treated by common methods such as coagulation, biodegradation, and meanwhile seldom studies on its treatment have been reported. Alizarin violet 3B is a common dye, which have been also used as a biological stain. They have different molecular structure, one is a basic cationic dye, and another is a sulfonate anionic dye.

Recently, our group and others have reported the photodegradation of Malachite Green [15,16] and Orange-II [17] in the Fenton-like system under visible irradiation. AO and

* Corresponding author. Present address: Institute of Photographic Chemistry, the Chinese Academy of Sciences, Beijing 100101, China. Fax: +86-10-64879375.
E-mail address: jczhao@ipc.ac.cn (J. Zhao).

1010-6030/00/$ – see front matter
PII: S1010-6030(00)00341-5

AV, one is an anionic dye and another one is a cationic dye, are difficult to degrade by common methods. In this paper, we present the results of the degradation of these two different dyes AO and AV in the Fenton-like system under visible irradiation and analyzed the intermediates formed during the degradation of AO by EPR, IR, GC–MS spectroscopy emphatically, and analyzed the ammonium ions formed. These results are very useful for us to understand the photodegradation and its mechanism of dyes under visible irradiation.

2. Experimental

Acridine orange monohydrochloride (AO) and alizarin violet 3B (AV), $FeCl_3 \cdot 6H_2O$, $FeSO_4 \cdot 7H_2O$, sodium dodecylbenzenesulfonate (DBS), sodium oxalate, H_2O_2 (30% aqueous solution) were of reagent grade and used without further purification. The spin trap 5,5-dimethyl-1-pyrroline-*N*-oxide (DMPO) was purchased from Sigma. Deionized and then doubly distilled water was used throughout the experiments.

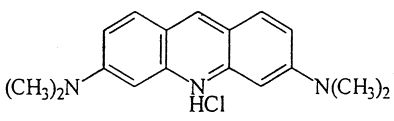

AO

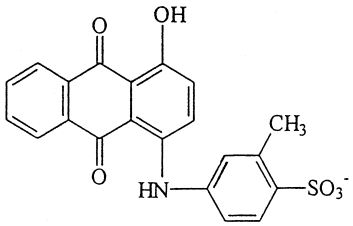

AV

Irradiation source was a 500 W halogen lamp equipped with a Pyrex glass cooling jacket with water circulation and a light filter (cutoff the light less than 470 nm wavelength). Solutions for irradiation were freshly prepared from air saturated stock solution of $FeCl_3$ at pH 1.9 and the dye stock solution, and then adjusted to desired pH values (initial pH 2.9) with HCl and NaOH solutions. All the irradiation experiments were carried out in a 60-ml Pyrex glass vessel. At given irradiation time intervals, the samples (3 ml) were taken out and then analyzed by observation of variations in UV–Vis spectra with a Perkin Elmer UV/Vis spectrophotometer. Total organic carbons (TOC) of the degraded solutions were measured with a Shimadzu 5000 TOC analyzer. EPR measurements were carried out with a Bruker model 300E EPR spectrometer equipped with a laser irradiation light source (355 and 532 nm) of a Quanty-Ray Nd:YAG system. BIOS-RAD FTS165 infrared spectroscopy and gas chromatography/mass spectroscopy (Trio-2000, equipped with a BPX70 column, size 28 m × 0.25 mm) were used to determine the intermediates formed in the degradation process. The samples for IR measurements were prepared as follows: after certain irradiation time, the reaction was stopped by addition of a NaOH solution to remove the remaining H_2O_2 and deposit Fe^{3+}. After removal of the sediment of $Fe(OH)_3$ by filtration, the filtrate was acidified with HCl and the H_2O in the filtrate was removed under reduced pressure (below 40°C), the residue with KBr as a solid support was used for IR experiments. The samples for GC–MS measurements were prepared through directly condensing the reaction solution under reduced pressure (below 40°C) and the remaining residue was dissolved in a mixed solvent methanol and DMSO for GC–MS experiments.

3. Results and discussion

3.1. The photocatalytic degradation of dyes

The UV–Vis spectrum of AO displays a maximum peak at 490 nm with a shoulder peak at 472 nm, which correspond to the monomer and dimer [18], respectively (see the inset of Fig. 1). The photodegradation of AO and its TOC changes of the systems are shown in Fig. 1. From that, we may find that the degradation rates of AO, AO/H_2O_2 or AO/Fe^{3+} systems (curves a–c) under visible irradiation were similar. The degradation rate in AO/Fe^{3+}/H_2O_2 system became slow in the dark (curve d) and meanwhile approximately displayed a zero-order reaction with a rate

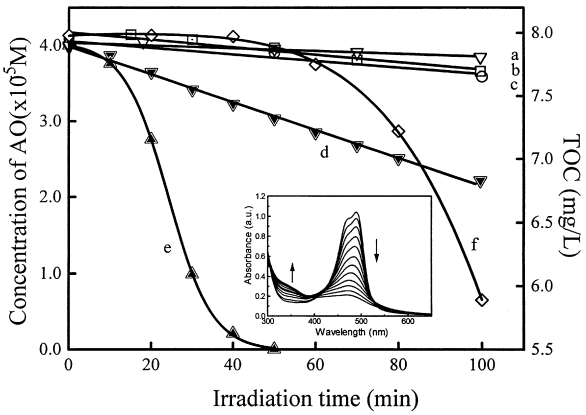

Fig. 1. The degradation of AO under different conditions: a, AO, visible irradiation; b, AO/H_2O_2, visible irradiation; c, AO/Fe^{3+}, visible irradiation; d, AO/Fe^{3+}/H_2O_2, dark reaction; e, AO/Fe^{3+}/H_2O_2, visible irradiation; f, TOC changes of system; e, the irradiation energy was 192 mW/cm^2. All the reactions were in pH 2.9, $Fe^{3+} = 8 \times 10^{-5}$ M; $H_2O_2 = 0.07$ M; AO (4×10^{-5} M). The condition of the inset figure is same as curve e.

constant $K = 3.5 \times 10^{-8}\,M\,s^{-1}$, but the degradation of AO in the Fe^{3+}/H_2O_2 system under visible irradiation (curve e) was much faster than that of it. Otherwise, the TOC change during the photo-Fenton degradation of AO was also examined as shown in Fig. 1 (curve f). In the system of AO (4×10^{-5} M), Fe^{3+} (8×10^{-5} M) and H_2O_2 (0.07 M), the TOC degradation reached 26.2 and 84.5% after 100 and 160 min of visible irradiation, respectively. During the initial period, both the degradation (curve e) and the mineralization (TOC changes, curve f) of AO had an induction period, after which both of them were accelerated. It indicated that visible irradiation could effectively enhance the degradation of AO. Additionally, the degradation of AO had an induction period and began with the decoloration (curve e). With the decoloration of AO, the structure of the dye molecule was destroyed. The dye was gradually oxidized into small molecular compounds and finally oxidized into water and mineralization products.

AV shows a maximum peak around 568 nm (see the inset of Fig. 2). Fig. 2 shows the degradation of AV under different conditions. The concentration of AV in the Fe^{3+}/H_2O_2 solution decreased rapidly under visible irradiation (curve e). Blank experiments revealed a much slower degradation rate for the AV only, AV/H_2O_2, or AV/Fe^{3+} solutions under visible irradiation. The degradation rate of AV in $Fe^{3+}/H_2O_2/AV$ system under visible irradiation was faster than that in the dark. The TOC change approximately showed a linear correlation with the reaction time within 160 min of visible irradiation (curve f), and the TOC degradation reached 46 and 87.5% at 100 and 160 min under visible irradiation, respectively. From the above results, it could be found that AV could also be degraded by the photo-Fenton method and visible irradiation could enhance the degradation of it.

Comparing the degradation between them, the point different is that the degradation process of AO exhibited an induction period but the degradation of AV did not.

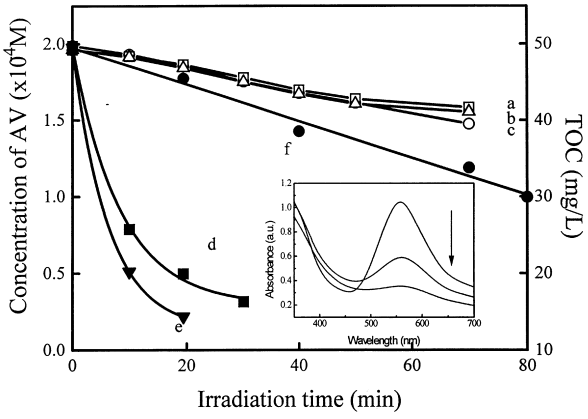

Fig. 2. The degradation of AV under different conditions: a, AV, visible light; b, AV/H_2O_2, visible light; c, AV/Fe^{3+}, visible light; d, $AV/Fe^{3+}/H_2O_2$, in the dark; e, $AV/Fe^{3+}/H_2O_2$, visible light; f, TOC changes of system e. The irradiation energy was 192 mW/cm^2. All the reactions were in pH 2.9, AV $= 2 \times 10^{-4}$ M, $Fe^{3+} = 2 \times 10^{-4}$ M, $H_2O_2 = 0.07$ M. The condition of the inset is same as that of curve e.

3.2. EPR measurements during the reaction of AO

The electron spin trapping technique is an effective method in identification of active radicals. In this work, we chose DMPO as the scavenger of radicals that was generated during the degradation of AO and AV. All the measured EPR-spectra of the below solutions under in situ laser irradiation ($\lambda = 532$ nm) exhibited a fourfold peak with the intensity ratio 1:2:2:1. This is the typical and characteristical EPR signal of DMPO–OH adduct. From the change of the intensity of hydroxyl radical, we may directly find the enhancement of visible irradiation (see Fig. 3(A)). These results indicate that hydroxyl radicals had been generated. The changes in intensity of signal of hydroxyl radical at different reaction times under visible irradiation are shown in Fig. 3(B), I_0 refers to the intensity of signal of hydroxyl radical at the beginning of the reaction (before irradiation). The intensity of signal of hydroxyl radical slightly

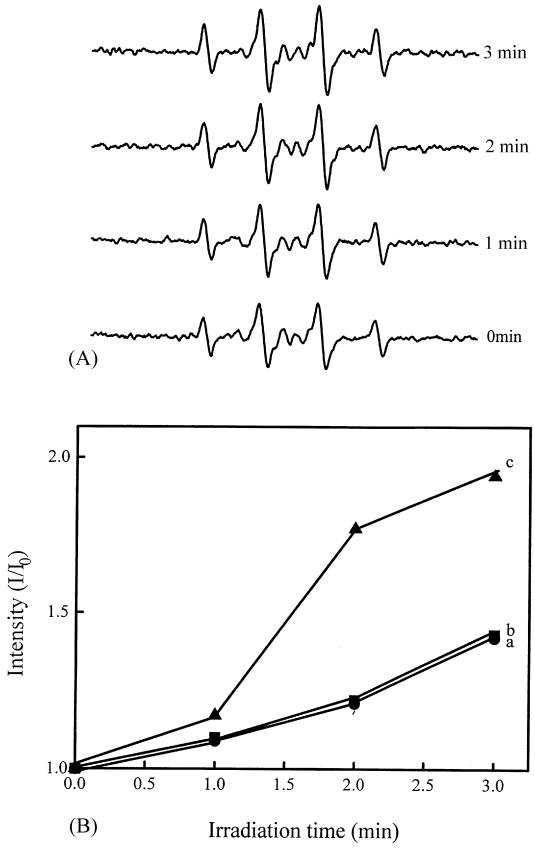

Fig. 3. (A) The EPR spectra of Fe^{3+}/H_2O_2 system under visible irradiation, 532 nm laser. The irradiation energy at 532 nm was 360 mJ/pulse, irradiation frequency was 10 Hz. The reaction was in pH 2.9, $Fe^{3+} = 5.73 \times 10^{-4}$ M, $H_2O_2 = 0.05$ M, AO $= 2.86 \times 10^{-4}$ M. (B) The changes of the intensities of hydroxyl radical signals under visible irradiation: a, Fe^{3+}/H_2O_2 system, 532 nm laser; b, $AO/Fe^{3+}/H_2O_2$ system in dark; c, $AO/Fe^{3+}/H_2O_2$ system, 532 nm laser. The irradiation energy at 532 nm was 360 mJ/pulse, irradiation frequency was 10 Hz. All the reactions were in pH 2.9, $Fe^{3+} = 5.73 \times 10^{-4}$ M, $H_2O_2 = 0.05$ M, AO $= 2.86 \times 10^{-4}$ M.

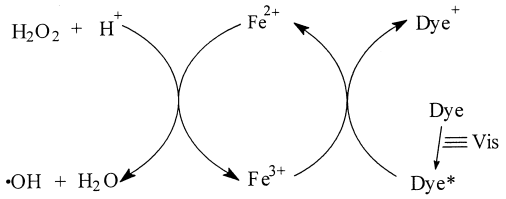

Scheme 1. A possible mechanism of production of hydroxyl radicals and the cycling of ferric/ferrous ions.

increased for Fe^{3+}/H_2O_2 system under visible irradiation or for Fe^{3+}/H_2O_2/AO in the dark (see curves a and b), but the intensities of hydroxyl radical signals in Fe^{3+}/H_2O_2/AO system had an apparent increase when the system was irradiated by visible light (see curve c). When AO was replaced by AV, the results were identical. These results indicate that visible irradiation can effectively accelerate the generation of hydroxyl radicals, a possible mechanism was that visible irradiation promoted the regeneration of Fe^{2+} (Eqs. (3) and (4) and Scheme 1), which accelerate the production of $^{\bullet}OH$ radicals [17]. Dye absorbs the visible light, and is excited into the high-energy state. When the excited dye molecule encounters the aqueous ferric ion, an electron in the excited dye molecule transfers into the ferric ion that further reduced into the ferrous ion. The reduced ferrous ion reacted with hydrogen peroxide, and further let hydrogen peroxide to decompose and generated hydroxyl radical. A similar mechanism has been proposed in our former work and demonstrated by Herrera [14,15,19].

$$\text{Dye} \rightarrow \text{Dye}^* \quad (3)$$

$$\text{Dye}^* + Fe^{3+} \rightarrow \text{Dye}^+ + Fe^{2+} \quad (4)$$

In order to further identify the roles of light irradiation and the dyes, we measured the EPR signals under similar conditions but with 355 nm laser irradiation, the results are shown in Fig. 4. When the solutions of both Fe^{3+}/H_2O_2 and

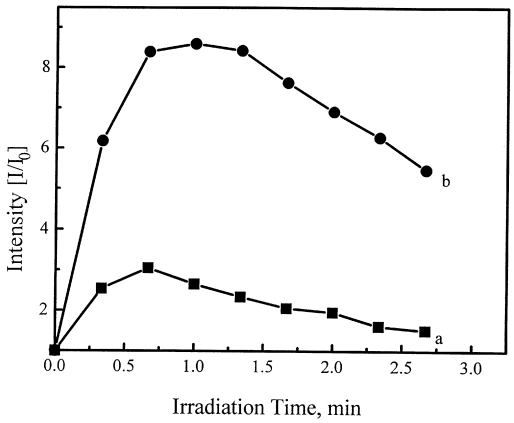

Fig. 4. The changes of the intensities of hydroxyl radical signals under UV irradiation: a, Fe^{3+}/H_2O_2 system, 355 nm laser; b, AO/Fe^{3+}/H_2O_2 system, 355 nm laser. The irradiation energy at 355 nm was 185 mJ/pulse, irradiation frequency was 10 Hz. All the reactions were in pH 2.9, $Fe^{3+} = 5.73 \times 10^{-4}$ M, $H_2O_2 = 0.05$ M, DMPO = 0.028 M.

Fe^{3+}/H_2O_2/AO (or AV) were irradiated by UV light, the intensities of EPR signals drastically increased (see curves a and b), since UV light irradiation may excite $Fe(OH)^{2+}$ to generate hydroxyl radicals and Fe^{2+} (see Eqs. (1) and (2)). Nevertheless, comparing curve a with curve b, we can also find that the generation rate of hydroxyl radicals in Fe^{3+}/H_2O_2/AO (or AV) was apparently much faster than that in Fe^{3+}/H_2O_2 under the same conditions. This clarifies that the dyes were excited and electron transfer between the dye and ferric ion took place, and further also improved the generation of hydroxyl radicals under UV irradiation.

3.3. The FT-IR analysis of the intermediates during the degradation of AO

In order to further research the degradation mechanism of the dyes, we first chose AO as the target pollutant and measured the infrared spectra of the intermediates produced at different reaction periods as shown in Fig. 5. In our experiment, we chose a high-content aqueous solution of AO in order to clearly observe the intermediates formed in the initial degradation. According to the IR spectrum of the AO sample (diagram a), the absorption peaks at 1636, 1354 and 1177 cm^{-1} are due to the stretching vibration of the frame of the conjugated ring, the stretching vibration of Ar–N bonds and the bending vibration of Ar–H bonds, respectively. From the measured results, we can also find that the characteristic peaks apparently changed as the reaction proceeded.

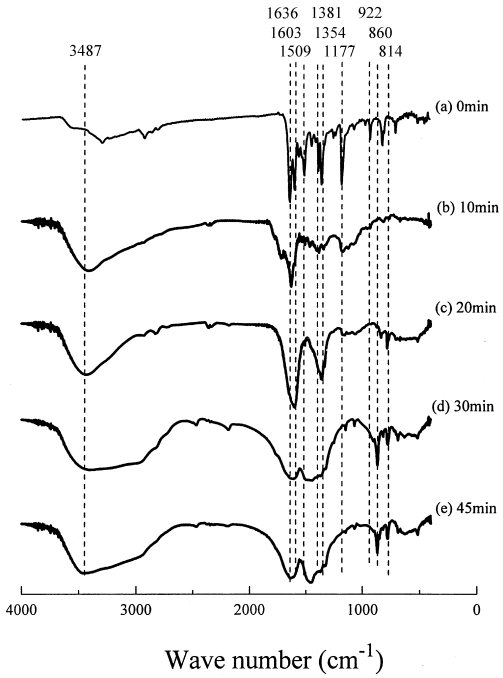

Fig. 5. IR spectra of the intermediates during the degradation of AO in AO/Fe^{3+}/H_2O_2 system under visible irradiation, reaction time: (a) 0 min; (b) 10 min; (c) 20 min; (d) 30 min; and (e) 45 min. All the reactions were in pH 2.9. $Fe^{3+} = 8 \times 10^{-5}$ M, $H_2O_2 = 0.07$ M, AO (4×10^{-5} M).

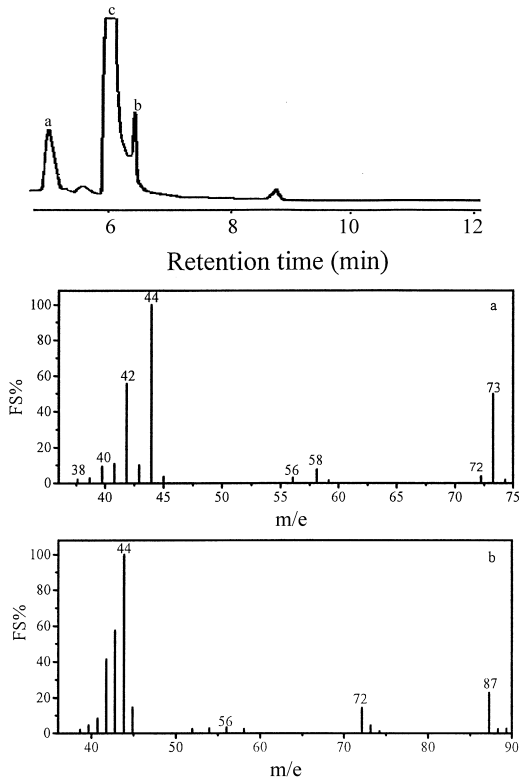

Fig. 6. GC–MS spectra of the intermediates during the degradation of AO in AO/Fe^{3+}/H_2O_2 system. The reaction was in pH 2.9 and the reaction time was 60 min. Signal c in the GC spectra is the peak of solvent DMSO.

When the reaction was carried out for 10 min, the peak of 1177 cm^{-1} apparently decreased and almost disappeared after 45 min. The absorption around 1636 cm^{-1} shifted to 1603 cm^{-1} and meanwhile its shape became wide, the one around 1354 cm^{-1} also became wide and strong. Furthermore, a wide absorption peak around 3487 cm^{-1}, which is due to the stretching vibration of O–H bond, apparently became strong. This indicates that the hydroxylated adducts were gradually formed. Additionally, the peak of 1701 cm^{-1} emerged and another new peak of 860 cm^{-1} also appeared. These changes indicated that the conjugated cycles were gradually hydroxylated by hydroxyl radicals and some compounds with carbonyl group were formed.

3.4. The GC–MS analysis of the intermediates during the degradation of AO

In order to understand the degradation path of the dyes, we determined the intermediates of the degradation of AO by GC–MS spectroscopy. The sample was the intermediates after 45 min of reaction. The measurement results are shown in Fig. 6. The top figure is the gas chromatography of the intermediates, in which several peaks emerged. Among the intermediates, *N*,*N*-dimethyl formamide (Fig. 6(a)) and *N*,*N*-dimethyl acetamide (Fig. 6(b)) were identified. This clarifies that *N*,*N*-dimethyl formamide and *N*,*N*-dimethyl acetamide formed during the degradation of AO.

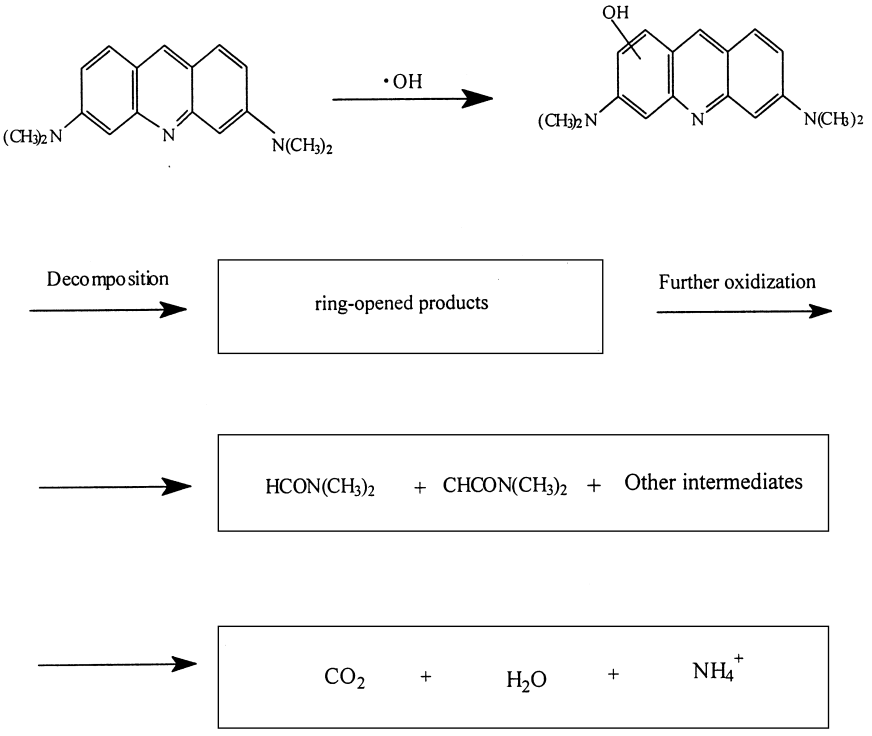

Scheme 2. A possible mechanism of degradation of AO in the photo-Fenton system under visible irradiation.

3.5. Degradation mechanism

Combining the analyses of the FT-IR and GC–MS spectroscopy with the results of EPR, it was indicated that the photo-Fenton degradation of AO under visible irradiation possibly initiated from the hydroxylation of the dye molecules by $^{\bullet}OH$ radical generated from the Fe^{2+}-assisted decomposition of H_2O_2 and the decoloration of the dye molecules, and meanwhile the conjugated rings of hydroxylated dye molecules opened. Finally the dye molecules were oxidized into water and the corresponding mineralized products (CO_2 and NH_4^+) via some intermediates such as *N*,*N*-dimethyl acetamide and *N*,*N*-dimethyl formamide (see Scheme 2). This degradation mechanism is different from the photocatalytic degradation of dyes [20].

4. Conclusion

The photodegradation of AO and AV with the photo-Fenton method was firstly reported. It was found that they can be effectively photodegraded into water and their corresponding mineralized products under visible irradiation. Hydroxyl radicals were generated under visible irradiation. Visible irradiation can apparently enhance the generation of $^{\bullet}OH$ radicals in the presence of the dyes and accelerate effectively the degradation of dyes themselves in the Fenton-like system, which provides an economical approach in treatment of dye pollutants, and played important roles in the degradation of dyes. During the degradation of AO, *N*,*N*-dimethyl formaldehyde and *N*,*N*-dimethyl acetamide were found.

Acknowledgements

This work was supported by the National Natural Science Foundation of China (No. 29877026, No. 29725715 and No. 29637010), the Foundation of China Academy of Sciences and National Committee of China Science and Technology.

References

[1] R. Zepp, B. Faust, J. Holgne, Environ. Sci. Technol. 26 (1992) 313.
[2] M. Halmann, J. Photochem. Photobiol. A 66 (1992) 215.
[3] J. Kiwi, C. Pulgarin, P. Peringer, M. Gratzel, Appl. Catal. B 3 (1993) 85.
[4] P. Pichat, Wat. Sci. Technol. 35 (1997) 73.
[5] A. Nedoloujko, J. Kiwi, J. Photochem. Photobiol. A 110 (1997) 149.
[6] V. Nadtochenko, J. Kiwi, Environ. Sci. Technol. 32 (1998) 3273.
[7] V. Nadtochenko, J. Kiwi, Environ. Sci. Technol. 32 (1998) 3282.
[8] J. Kiwi, C. Pulgrin, P. Peringer, Appl. Catal. B 3 (1994) 335.
[9] R. Chen, J. Pignatello, Environ. Sci. Technol. 31 (1997) 2399.
[10] V. Nadtochenko, J. Kiwi, J. Photochem. Photobiol. A 99 (1996) 145.
[11] P. Maletzky, R. Bauer, Chemosphere 37 (1998) 899.
[12] V. Nadochenko, J. Kiwi, J. Chem. Soc., Faraday Trans. 93 (1997) 2373.
[13] J. Pignatello, Environ. Sci. Technol. 26 (1992) 944.
[14] A. S-Amiri, J.R. Bolton, S.R. Cater, J. Adv. Oxid. Technol. 1 (1996) 18.
[15] K. Wu, Y. Xie, J. Zhao, H. Hidaka, J. Mol. Catal. A 144 (1999) 77.
[16] K. Wu, T. Zhang, J. Zhao, H. Hidaka, Chem. Lett. 6 (1998) 857.
[17] J. Bandara, C. Morrison, J. Kiwi, C. Pulgrin, P. Peringer, J. Photochem. Photobiol. A 99 (1996) 57.
[18] S. Moulik, S. Ghosh, A. Das, Indian J. Chem. A 14 (1976) 302.
[19] F. Herrara, J. Kiwi, A. Lopez, V. Nadtochenko, Environ. Sci. Technol. 33 (1999) 3145.
[20] J. Zhao, T. Wu, K. Wu, H. Hidaka, N. Serpone, Environ. Sci. Technol. 32 (1998) 2394.